

Control of xenon oscillations in Advanced Heavy Water Reactor via two-stage decomposition



R.K. Munje^a, J.G. Parkhe^b, B.M. Patre^{b,*}

^aK.K. Wagh Institute of Engineering Education and Research, Nashik 422 003, India

^bS.G.S. Institute of Engineering and Technology, Nanded 431 606, India

ARTICLE INFO

Article history:

Received 28 November 2013

Received in revised form 20 November 2014

Accepted 21 November 2014

Keywords:

Advanced Heavy Water Reactor

Singular perturbation

Spatial oscillations

Two-stage decomposition

ABSTRACT

Xenon induced spatial oscillations developed in large nuclear reactors, like Advanced Heavy Water Reactor (AHWR) need to be controlled for safe operation. Otherwise, a serious situation may arise in which different regions of the core may undergo variations in neutron flux in opposite phase. If these oscillations are left uncontrolled, the power density and rate of change of power at some locations in the reactor core may exceed their respective thermal limits, resulting in fuel failure. In this paper, a state feedback based control strategy is investigated for spatial control of AHWR. The nonlinear model of AHWR including xenon and iodine dynamics is characterized by 90 states, 5 inputs and 18 outputs. The linear model of AHWR, obtained by linearizing the nonlinear equations is found to be highly ill-conditioned. This higher order model of AHWR is first decomposed into two comparatively lower order subsystems, namely, 73rd order 'slow' subsystem and 17th order 'fast' subsystem using two-stage decomposition. Composite control law is then derived from individual subsystem feedback controls and applied to the vectorized nonlinear model of AHWR. Through the dynamic simulations it is observed that the controller is able to suppress xenon induced spatial oscillations developed in AHWR and the overall performance is found to be satisfactory.

© 2014 Elsevier Ltd. All rights reserved.

1. Introduction

The analysis and control of large scale systems has always been a complicated task due to high order nature and interacting dynamic phenomena of widely different speeds, which gives rise to time-scales. Such systems are extensively studied in control theory by singular perturbations and time-scale methods. Excellent survey of control theory applications of singular perturbations is given by Kokotovic et al. (1976). Another survey on singular perturbation in modeling, analysis and design of nonlinear, stochastic and large scale decentralized system is presented by Saksena et al. (1984). Singular perturbation methods have successfully been used in control application to deal with large scale system, by which the system is decoupled into 'slow' and 'fast' subsystems (Kokotovic et al., 1976). These methods work by decoupling the slow and fast varying phenomena, which leads to model order reduction. This decoupling is achieved either by quasi-steady-state method (Gajic and Lim, 2001) or direct block diagonalization (Naidu, 1988; Ladde and Siljak, 1983). The quasi-steady-state method is

an effective method for decoupling a large order system into slow and fast subsystems for sufficiently small perturbation parameter ϵ . However, for real systems, like nuclear reactor the perturbation parameter is not zero. As a result, when using quasi-steady-state method the eigenvalues of the slow and fast subsystems are no longer in the same position as the eigenvalues of the full order system. To overcome this, block-diagonalization procedure (Phillips, 1980; Naidu, 1988) can be employed. In this method, exact decoupling is achieved. Feedback control designs for such systems may then proceed for each subsystem and the results are combined to yield a "composite" feedback control for the original system. The cases of state feedback control are treated in Chow and Kokotovic (1984), Phillips (1980), Saberi and Khalil (1985), and Suzuki (1981). Chow and Kokotovic (Chow and Kokotovic, 1984) have developed the procedure for linear systems and applied it to linear quadratic optimal designs. A cost functional, extracted from the cost functional for the full system, is associated with each subsystem. They have also shown that the composite state feedback control is stabilizing and near-optimal with the optimal cost. Suzuki (1981) has shown that controllability and stabilizability properties of the slow subsystem are invariant with respect to the feedback from fast state variables. This property is further explored by Saberi and Khalil (1985). They showed that the closed

* Corresponding author. Tel.: +91 2462 269341; fax: +91 2462 229236.

E-mail addresses: ravimunjje@yahoo.co.in (R.K. Munje), jgparkhe@gmail.com (J.G. Parkhe), bmpatre@ieee.org (B.M. Patre).

Nomenclature

Notations

C	precursor concentration
α	coupling coefficient
E_{eff}	thermal energy liberated/fission, J
β	delayed neutron fraction
\mathbf{E}_n	identity matrix of dimension n
γ	fraction fission yield
H	position of regulating rod, % in
λ	Decay constant
I	iodine concentration
ℓ	the prompt neutron life-time, s
P	fission power, W
ρ	reactivity, k
V	volume, m ³
σ_a	microscopic absorption cross-section, cm ²
X	xenon concentration
Σ_a	macroscopic absorption cross-section, cm ⁻¹
h	enthalpy, kJ/kg
Σ_f	macroscopic fission cross-section, cm ⁻¹
q	mass flow rate, kg/s
κ	constant of regulating rod position

v	voltage signal to RR drive, V
δ	deviation parameter
x	exit mass quality
φ	eigenvalue

Subscripts

C	precursor
f	fast, feed water, fission
H	position of regulating rod
i, j	node number
I	iodine
k	regulating rod number
P	power
s	slow, steam
X	xenon
w	water
c	vaporization
gp	global power
d	downcomer
sp	spatial power

loop slow subsystem is invariant with respect to any feedback function which preserves the equilibrium of the fast subsystem as an isolated equilibrium of fast subsystem obtained with $\epsilon = 0$. Further, two-stage eigenvalue placement via explicitly invertible transformation is suggested by Phillips (1980).

In the context of power distribution control in large nuclear reactors, like Advanced Heavy Water Reactor (AHWR) and Pressurized Heavy Water Reactor (PHWR), it is worth mentioning that the models of these reactors belong to singularly perturbed systems. These reactors exhibit slow as well as fast varying dynamical modes, which causes ill-conditioning of the problem. Moreover, the physical dimensions of these reactors are large compared to neutron migration length. Hence, they are susceptible to xenon induced spatial oscillations. Spatial oscillations in neutron flux distribution resulting from xenon reactivity feedback are a matter of concern in large nuclear reactors. If the spatial oscillations in power distribution are not controlled, power density and rate of change of power at some locations in the reactor core may exceed limits of fuel failure (Duderstadt and Hamilton, 1975). Spatial control means to suppress xenon oscillations from growing. Control of xenon oscillations developed in AHWR has been attempted by Shimjith et al. (2011a), Munje et al. (2014a) using static output feedback technique. However, static output feedback does not guarantee stability of closed loop system. As an extension to this, a state feedback based two-time-scale approach for PHWR is given by Tiwari et al. (1996) and three-time-scale approach for AHWR is presented by Shimjith et al. (2011b). In these, quasi-steady-state method is used to decouple the higher order system into lower order subsystems. Nevertheless, the practical implementation of such a state feedback based controller demands a state observer of large order. Hence, a linear observer has been suggested for PHWR in Tiwari and Bandyopadhyay (1998). Further, the observer based design increases the implementation cost and reduces the reliability of the control system. To overcome this, a three-time-scale based Fast Output Sampling (FOS) controller is investigated in Shimjith et al. (2011c). A similar kind of approach for two-time-scale system is also suggested by Munje et al. (2013a) for AHWR system. In FOS, control signal is generated as a linear combination of a number of output samples collected in one sampling interval, where input sampling time is larger compared

to output. For example in Shimjith et al. (2011c), sampling time for spatial control component of input is taken as 60 s and in Munje et al. (2013a) it is taken as 54 s. However, for practical reactor control to work with larger sampling time is not desirable, because in small time, reactor system can undergo a considerable change. Hence, Periodic Output Feedback (POF) based controller for three-time-scale system of AHWR is presented in Munje et al. (2014b) with sampling period of 2 s. A two-time-scale decomposition approach using POF is documented in Patre et al. (1997), Tiwari et al. (2000). These multirate output feedback based controllers (i.e. FOS and POF) have their own advantages, but they lack robustness. Moreover, these methods may not work satisfactorily in the presence of disturbance, parameter variations and perturbations in the operating conditions. Recently, Munje et al. (2013b) have explored state feedback based robust Sliding Mode Control (SMC) technique to AHWR and it is shown that, better results are obtained compared to other control techniques. Furthermore, a single-input fuzzy logic controller (Londhe et al., 2014) is also proposed for spatial control of AHWR.

In this paper, singularly perturbed structure of Advanced Heavy Water Reactor is exploited, to decouple it into a slow subsystem of 73rd order and fast subsystem of 17th order, using the method of Phillips (1980) and a composite controller is designed for suppressing xenon induced spatial oscillations. In contrast to the earlier work of Shimjith et al. (2011b), where quasi-steady-state method was used to obtain three subsystems, this two-stage decomposition method provides higher degree of accuracy. Moreover, the comparison of results, helps to understand the effect of different model order reduction methods. Organization of the paper is as follows. In Section 2 brief overview of AHWR system is given. Control design is proposed in Section 3. In Section 4 application to AHWR system is presented followed by conclusion in Section 5.

2. Overview of AHWR

2.1. Introduction

In India, Advanced Heavy Water Reactor, a 920 MW (thermal), vertical pressure tube type reactor has been designed. It is moderated by heavy water, cooled by boiling light water and

fueled with (Th–²³³U) O₂ and (Th–Pu) O₂ pins (Sinha and Kakodkar, 2006). The reactivity control devices in AHWR consist of eight absorber rods (ARs), eight shim rods (SRs) and eight regulating rods (RRs). For spatial control system design of AHWR, a very extensive derivation of AHWR mathematical model is obtained in Shimjith et al. (2008, 2010) and the same has been used here for the study carried out in this paper. However, for brevity the model is discussed briefly in the following.

2.2. Core neutronics model

The AHWR core is considered to be divided in 17 relatively large nodes as shown in Fig. 1. The following nonlinear equations constitute the core neutronics model

$$\frac{dP_i}{dt} = (\rho_i - \alpha_{ii} - \beta) \frac{P_i}{\ell} + \sum_{j=1}^{17} \alpha_{ji} \frac{P_j}{\ell} + \lambda C_i, \quad (1)$$

$$\frac{dC_i}{dt} = \frac{\beta}{\ell} P_i - \lambda C_i, \quad (2)$$

$$\frac{dI_i}{dt} = \gamma_i \Sigma_{fi} P_i - \lambda_i I_i, \quad (3)$$

$$\frac{dX_i}{dt} = \gamma_X \Sigma_{fi} P_i + \lambda_i I_i - (\lambda_X + \bar{\sigma}_{Xi} P_i) X_i, \quad (4)$$

$$\frac{dH_k}{dt} = \kappa v_k, \quad k = 2, 4, 6, 8; \quad i = 1, 2, \dots, 17 \quad (5)$$

where α_{ji} and α_{ii} denote the coupling coefficients between j th and i th nodes and self coupling coefficients of i th node respectively. $\bar{\sigma}_{Xi} = \sigma_{Xi}/E_{eff} \Sigma_{fi} V_i$ and v_k is control signal applied to the RR drive and κ is a constant having value 0.56. For various notations refer nomenclature.

2.3. Thermal hydraulics model

The thermal hydraulics model (Shimjith et al., 2008) derived from Astrom and Bell (2000) is given by

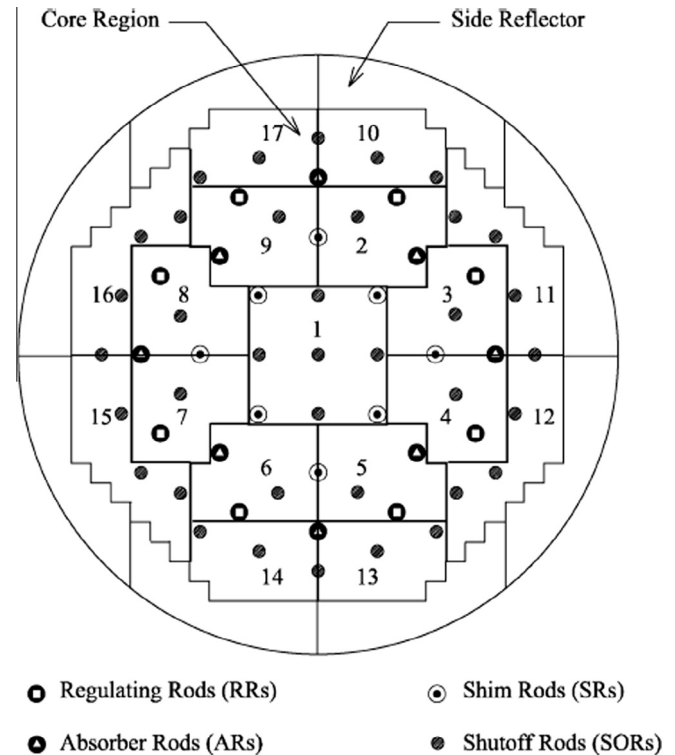


Fig. 1. 17 nodes AHWR scheme.

$$e_{vx_i} \frac{dx_i}{dt} = P_i - q_{d_i}(h_w - h_d) - q_{d_i} x_i h_c, \quad i = 1, 2, \dots, 17; \quad (6)$$

$$e_{xh} \frac{dh_d}{dt} = q_f(\hat{k}_2 h_f - \hat{k}_1) - q_d(\hat{k}_2 h_d - \hat{k}_1) \quad (7)$$

where, $\hat{k}_2 = \frac{h_c}{h_w}$ and $\hat{k}_1 = h_w \hat{k}_2$. Values of e_{vx_i} , e_{xh} , neutronic parameters, nodal volumes and cross-sections, nodal powers and coolant flow rates under full power operation and coupling coefficients are given in Shimjith et al. (2011a).

2.4. Reactivity feedbacks

The reactivity term ρ_i in (1) is expressed as $\rho_i = \rho_{iu} + \rho_{ix} + \rho_{iz}$, where ρ_{iu} , ρ_{ix} and ρ_{iz} are the reactivity feedbacks due to the control rods, xenon and coolant void fraction respectively. The reactivity contributed by the movement of the RRs is expressed as

$$\rho_{iu} = \begin{cases} (-10.234H_i + 676.203) \times 10^{-6}, & \text{if } i = 2, 4, 6, 8. \\ 0 & \text{elsewhere.} \end{cases}$$

The xenon reactivity feedback in node i can be expressed as

$$\rho_{ix} = -\frac{\bar{\sigma}_{Xi} X_i}{\Sigma_{ai}}, \quad i = 1, 2, \dots, 17.$$

The reactivity contribution by the coolant void fraction is

$$\rho_{iz} = -5 \times 10^{-3} (9.2832x_i^5 - 27.7192x_i^4 + 31.7643x_i^3 - 17.7389x_i^2 + 5.2308x_i + 0.0792), \quad i = 1, 2, \dots, 17.$$

2.5. Linearization and state space representation

The set of equations given by (1)–(7) can be linearized around steady state operating conditions (H_{k_0} , X_{i_0} , I_{i_0} , h_{d_0} , C_{i_0} , x_{i_0} , P_{i_0}) and the linear equations so obtained can be represented in standard state space form. For this, define the state vector as

$$\mathbf{z} = [\mathbf{z}_H^T \quad \mathbf{z}_X^T \quad \mathbf{z}_I^T \quad \delta h_d \quad \mathbf{z}_C^T \quad \mathbf{z}_x^T \quad \mathbf{z}_p^T]^T \quad (8)$$

where $\mathbf{z}_H = [\delta H_2 \quad \delta H_4 \quad \delta H_6 \quad \delta H_8]^T$ and the rest $\mathbf{z}_\xi = [(\delta \xi_1/\xi_{1_0}) \dots (\delta \xi_{17}/\xi_{17_0})]^T$, $\xi = X, I, C, x, P$, in which δ denotes the deviation from respective steady state value of the variable.

Likewise, define the input vector as $\mathbf{u} = [\delta v_2 \quad \delta v_4 \quad \delta v_6 \quad \delta v_8]^T$ and output vector as $\mathbf{y} = [y_g \quad y_1 \quad \dots \quad y_{17}]^T$ where $y_g = \sum_{i=1}^{17} \frac{\delta P_i}{P_{i_0}}$ and

$y_i = \frac{\delta P_i}{P_{i_0}}$ correspond to normalized total reactor power and nodal powers respectively. Then the system given by (1)–(7) can be expressed in standard linear state space form as

$$\dot{\mathbf{z}} = \mathbf{A}\mathbf{z} + \mathbf{B}\mathbf{u} + \mathbf{B}_{fw} \delta q_{fw}, \quad (9)$$

$$\mathbf{y} = \mathbf{M}\mathbf{z} \quad (10)$$

where q_{fw} is feed water flow rate. Matrices \mathbf{A} , \mathbf{B} , \mathbf{B}_{fw} and \mathbf{M} are given in Shimjith et al. (2011a). Eigenvalues of \mathbf{A} fall in two distinct clusters. First cluster has 73 eigenvalues ranging from -1.8395×10^{-1} to 3.9654×10^{-6} and the second one is of 17 eigenvalues ranging from -2.7626×10^2 to -7.2516 . Six eigenvalues of \mathbf{A} have their real parts positive while four eigenvalues are at the origin (grouped in first cluster), which indicates instability. Hence, it is necessary to design an effective controller to maintain the total power of the reactor while the xenon induced oscillations are being controlled.

3. Control design

Consider the linear time-invariant controllable and observable continuous-time system of order n as

$$\begin{bmatrix} \dot{\mathbf{z}}_1 \\ \dot{\mathbf{z}}_2 \end{bmatrix} = \begin{bmatrix} \mathbf{A}_{11} & \mathbf{A}_{12} \\ \frac{\mathbf{A}_{21}}{\epsilon} & \frac{\mathbf{A}_{22}}{\epsilon} \end{bmatrix} \begin{bmatrix} \mathbf{z}_1 \\ \mathbf{z}_2 \end{bmatrix} + \begin{bmatrix} \mathbf{B}_1 \\ \frac{\mathbf{B}_2}{\epsilon} \end{bmatrix} \mathbf{u} \quad (11)$$

where $\mathbf{z}_1 \in \mathbb{R}^{n_1}$, $\mathbf{z}_2 \in \mathbb{R}^{n_2}$ denote states such that $n_1 + n_2 = n$, the matrices \mathbf{A}_{ij} and \mathbf{B}_i are of appropriate dimensionality, parameter $\epsilon > 0$ is a scalar representing the speed ratio of the slow versus fast phenomenon and let

$$\mathbf{A} = \begin{bmatrix} \mathbf{A}_{11} & \mathbf{A}_{12} \\ \frac{\mathbf{A}_{21}}{\epsilon} & \frac{\mathbf{A}_{22}}{\epsilon} \end{bmatrix}, \quad \mathbf{B} = \begin{bmatrix} \mathbf{B}_1 \\ \frac{\mathbf{B}_2}{\epsilon} \end{bmatrix}, \quad \mathbf{z} = \begin{bmatrix} \mathbf{z}_1 \\ \mathbf{z}_2 \end{bmatrix}.$$

The model represented by (11) is a standard singularly perturbation model extensively studied in the control literature. As the parameter ϵ tends to zero, the solution behaves non-uniformly, producing so called singularly perturbed stiff problem. Suppose $\varphi(\mathbf{A})$ be the eigenvalues of matrix \mathbf{A} arranged in increasing order of absolute values as

$$\varphi(\mathbf{A}) = \{ \varphi_1, \varphi_2, \dots, \varphi_{n_1}, \varphi_{n_1+1}, \dots, \varphi_n \}$$

where

$$0 \leq |\varphi_1| < |\varphi_2| < \dots < |\varphi_{n_1}| \ll |\varphi_{n_1+1}| < \dots < |\varphi_n|.$$

Thus the system (11) has n_1 dominant (slow) modes and n_2 non-dominant (fast) modes.

3.1. Two-stage decomposition

The basic idea of using the two-stage decomposition approach in generating lower order models is to decouple the dominant modes from non-dominant modes. This is performed through use of two-stage linear transformation. The first stage is to apply the change of variables

$$\begin{bmatrix} \mathbf{z}_1 \\ \mathbf{z}_f \end{bmatrix} = \begin{bmatrix} \mathbf{E}_{n_1} & \mathbf{0} \\ \mathbf{L} & \mathbf{E}_{n_2} \end{bmatrix} \begin{bmatrix} \mathbf{z}_1 \\ \mathbf{z}_2 \end{bmatrix} = \mathbf{T}_1 \begin{bmatrix} \mathbf{z}_1 \\ \mathbf{z}_2 \end{bmatrix} \quad (12)$$

to system (11). Here \mathbf{E}_{n_1} and \mathbf{E}_{n_2} are respectively n_1 and n_2 identity matrices and $(n_2 \times n_1)$ matrix \mathbf{L} satisfies

$$\epsilon \mathbf{L} \mathbf{A}_{11} + \mathbf{A}_{21} - \epsilon \mathbf{L} \mathbf{A}_{12} \mathbf{L} - \mathbf{A}_{22} \mathbf{L} = \mathbf{0}. \quad (13)$$

Then system (11) transforms into

$$\begin{bmatrix} \dot{\mathbf{z}}_1 \\ \dot{\mathbf{z}}_f \end{bmatrix} = \begin{bmatrix} \mathbf{A}_s & \mathbf{A}_{12} \\ \mathbf{0} & \frac{\mathbf{A}_f}{\epsilon} \end{bmatrix} \begin{bmatrix} \mathbf{z}_1 \\ \mathbf{z}_f \end{bmatrix} + \begin{bmatrix} \mathbf{B}_s \\ \frac{\mathbf{B}_f}{\epsilon} \end{bmatrix} \mathbf{u} \quad (14)$$

where

$$\mathbf{A}_s = \mathbf{A}_{11} - \mathbf{A}_{12} \mathbf{L}, \quad \mathbf{A}_f = \mathbf{A}_{22} + \epsilon \mathbf{L} \mathbf{A}_{12}, \quad \mathbf{B}_s = \mathbf{B}_1 + \epsilon \mathbf{L} \mathbf{B}_1.$$

If \mathbf{A}_{22} is invertible, unique solution of \mathbf{L} in (13) can be determined by iterative procedure. Now the second linear transformation is applied as

$$\begin{bmatrix} \mathbf{z}_s \\ \mathbf{z}_f \end{bmatrix} = \begin{bmatrix} \mathbf{E}_{n_1} & -\epsilon \mathbf{N} \\ \mathbf{0} & \mathbf{E}_{n_2} \end{bmatrix} \begin{bmatrix} \mathbf{z}_1 \\ \mathbf{z}_f \end{bmatrix} = \mathbf{T}_2 \begin{bmatrix} \mathbf{z}_1 \\ \mathbf{z}_f \end{bmatrix} \quad (15)$$

to system (14) and choose $(n_1 \times n_2)$ matrix \mathbf{N} such that

$$\mathbf{A}_{12} - \mathbf{N} \mathbf{A}_{22} - \epsilon \mathbf{N} \mathbf{L} \mathbf{A}_{12} + \epsilon (\mathbf{A}_{11} - \mathbf{A}_{12} \mathbf{L}) \mathbf{N} = \mathbf{0}. \quad (16)$$

Then system (14) is transformed into

$$\begin{bmatrix} \dot{\mathbf{z}}_s \\ \dot{\mathbf{z}}_f \end{bmatrix} = \begin{bmatrix} \mathbf{A}_s & \mathbf{0} \\ \mathbf{0} & \frac{\mathbf{A}_f}{\epsilon} \end{bmatrix} \begin{bmatrix} \mathbf{z}_s \\ \mathbf{z}_f \end{bmatrix} + \begin{bmatrix} \mathbf{B}_s \\ \frac{\mathbf{B}_f}{\epsilon} \end{bmatrix} \mathbf{u} \quad (17)$$

where

$$\mathbf{B}_s = \mathbf{B}_1 - \mathbf{N} \mathbf{B}_f.$$

Thus, the application of two-stage linear transformation results in decoupling of system (11) into separate slow and fast subsystems in (17) from where the slow and fast variables \mathbf{z}_s and \mathbf{z}_f can be solved independently. Also, the magnitude of the largest eigenvalue of \mathbf{A}_s is much smaller than the magnitude of the smallest eigenvalue of $\frac{\mathbf{A}_f}{\epsilon}$, i.e.

$$\max |\varphi(\mathbf{A}_s)| \ll \min \left| \varphi \left(\frac{\mathbf{A}_f}{\epsilon} \right) \right|.$$

The transformations (12) and (15) relate the slow and fast variables \mathbf{z}_s and \mathbf{z}_f with the original variables \mathbf{z}_1 and \mathbf{z}_2 as

$$\dot{\mathbf{z}} = \mathbf{T} \dot{\mathbf{z}} \quad (18)$$

where $\dot{\mathbf{z}} = \begin{bmatrix} \dot{\mathbf{z}}_s^T & \dot{\mathbf{z}}_f^T \end{bmatrix}^T$, $\mathbf{z} = \begin{bmatrix} \mathbf{z}_1^T & \mathbf{z}_2^T \end{bmatrix}^T$ and $\mathbf{T} = \mathbf{T}_2 \mathbf{T}_1$.

Table 1
Eigenvalues of slow subsystem.

Sr. No.	Eigenvalues	Sr. No.	Eigenvalues	Sr. No.	Eigenvalues
1–3	0	33	-1.5717×10^{-4}	54	-6.2608×10^{-2}
4	-2.6799×10^{-5}	34	-1.6524×10^{-4}	55	-6.2865×10^{-2}
5	-3.7781×10^{-5}	35	-1.6653×10^{-4}	56	-6.2893×10^{-1}
6	-3.7993×10^{-5}	36	-1.7308×10^{-4}	57	-1.1715×10^{-1}
7	-4.0124×10^{-5}	37	-1.8807×10^{-4}	58	-1.4712×10^{-1}
8	-4.152×10^{-5}	38	-1.8870×10^{-2}	59	-1.4713×10^{-1}
9	-4.2044×10^{-5}	39	-5.2501×10^{-2}	60	-1.4809×10^{-1}
10	-4.4204×10^{-5}	40	-1.5867×10^{-2}	61	-1.485×10^{-1}
11	-4.7371×10^{-5}	41	-5.0954×10^{-2}	62	-1.5580×10^{-1}
12	-4.8866×10^{-5}	42	-5.1159×10^{-2}	63	-1.5585×10^{-1}
13–14	$(-7.747 \pm j 2.9929) \times 10^{-5}$	43	-5.773×10^{-2}	64	-1.5662×10^{-1}
15–16	$(-7.3359 \pm j 3.9319) \times 10^{-5}$	44	-5.7893×10^{-2}	65	-1.5585×10^{-1}
17–18	$(-6.5952 \pm j 5.4785) \times 10^{-5}$	45	-5.9707×10^{-2}	66	-1.5662×10^{-1}
19–20	$(-6.4855 \pm j 5.3109) \times 10^{-5}$	46	-5.9723×10^{-2}	67	-1.5761×10^{-1}
21–22	$(-3.9003 \pm j 8.9009) \times 10^{-5}$	47	-6.0344×10^{-2}	68	-1.6325×10^{-1}
23–24	$(-3.7785 \pm j 7.6475) \times 10^{-5}$	48	-6.0642×10^{-2}	69	-1.6405×10^{-1}
25–26	$(-3.5380 \pm j 7.7343) \times 10^{-5}$	49	-6.1848×10^{-2}	70	-1.8037×10^{-1}
27–28	$(8.8268 \pm j 2.1800) \times 10^{-5}$	50	-6.1942×10^{-2}	71	-1.8049×10^{-1}
29–30	$(8.0470 \pm j 3.9864) \times 10^{-5}$	51	-6.22×10^{-2}	72	-1.8122×10^{-1}
31	-1.4107×10^{-4}	52	-6.238×10^{-2}	73	-1.8402×10^{-1}
32	-1.4532×10^{-4}	53	-6.2458×10^{-2}		

3.2. Composite control law

The complete controllability of (11) implies the same for the subsystems in (17), i.e. for the pairs $(\mathbf{A}_s, \mathbf{B}_s)$ and $(\mathbf{A}_f, \mathbf{B}_f)$. Now, in order to design the state feedback for system (11), a two-step procedure is used. The input \mathbf{u} is represented as $\mathbf{u} = \mathbf{u}_s + \mathbf{u}_f$. The input \mathbf{u}_s is computed as

$$\mathbf{u}_s = [\mathbf{K}_s \quad \mathbf{0}] \begin{bmatrix} \mathbf{z}_s \\ \mathbf{z}_f \end{bmatrix} \quad (19)$$

where \mathbf{K}_s is $(m \times n_1)$ feedback gain matrix to place eigenvalues of $(\mathbf{A}_s + \mathbf{B}_s \mathbf{K}_s)$ at n_1 desired locations. Substituting the value of \mathbf{u}_s from (19) into (17) yields

$$\begin{bmatrix} \dot{\mathbf{z}}_s \\ \dot{\mathbf{z}}_f \end{bmatrix} = \begin{bmatrix} \mathbf{A}_s + \mathbf{B}_s \mathbf{K}_s & \mathbf{0} \\ \frac{\mathbf{B}_f \mathbf{K}_s}{\epsilon} & \frac{\mathbf{A}_f}{\epsilon} \end{bmatrix} \begin{bmatrix} \mathbf{z}_s \\ \mathbf{z}_f \end{bmatrix} + \begin{bmatrix} \mathbf{B}_s \\ \frac{\mathbf{B}_f}{\epsilon} \end{bmatrix} \mathbf{u}_f. \quad (20)$$

Now again, using transformation

$$\begin{bmatrix} \mathbf{z}_s \\ \mathbf{g}_f \end{bmatrix} = \begin{bmatrix} \mathbf{E}_{n1} & \mathbf{0} \\ \mathbf{U} & \mathbf{E}_{n2} \end{bmatrix} \begin{bmatrix} \mathbf{z}_s \\ \mathbf{z}_f \end{bmatrix} = \mathbf{T}_3 \begin{bmatrix} \mathbf{z}_s \\ \mathbf{z}_f \end{bmatrix} \quad (21)$$

system (20) is transformed into

$$\begin{bmatrix} \dot{\mathbf{z}}_s \\ \dot{\mathbf{g}}_f \end{bmatrix} = \begin{bmatrix} \mathbf{A}_s + \mathbf{B}_s \mathbf{K}_s & \mathbf{0} \\ \mathbf{0} & \frac{\mathbf{A}_f}{\epsilon} \end{bmatrix} \begin{bmatrix} \mathbf{z}_s \\ \mathbf{g}_f \end{bmatrix} + \begin{bmatrix} \mathbf{B}_s \\ \frac{\mathbf{B}_f}{\epsilon} \end{bmatrix} \mathbf{u}_f \quad (22)$$

where $\bar{\mathbf{B}}_f = \mathbf{B}_f + \epsilon \mathbf{U} \mathbf{B}_s$ and $(n_2 \times n_1)$ matrix \mathbf{U} satisfies

$$\epsilon \mathbf{U} (\mathbf{A}_s + \mathbf{B}_s \mathbf{K}_s) - \mathbf{A}_f \mathbf{U} + \mathbf{B}_f \mathbf{K}_s = \mathbf{0}. \quad (23)$$

As systems (20) and (22) are related via transformation (21), pair $(\mathbf{A}_f, \mathbf{B}_f)$ is also controllable. Therefore, the second input \mathbf{u}_f is selected as

$$\mathbf{u}_f = [\mathbf{0} \quad \mathbf{K}_f] \begin{bmatrix} \mathbf{z}_s \\ \mathbf{g}_f \end{bmatrix} \quad (24)$$

where \mathbf{K}_f is $(m \times n_2)$ feedback gain matrix to place eigenvalues of $(\frac{\mathbf{A}_f + \bar{\mathbf{B}}_f \mathbf{K}_f}{\epsilon})$ at n_2 desired locations. Closed loop system, obtained after application of \mathbf{u}_f , in (24) to (22) is given by

$$\begin{bmatrix} \dot{\mathbf{z}}_s \\ \dot{\mathbf{g}}_f \end{bmatrix} = \begin{bmatrix} \mathbf{A}_s + \mathbf{B}_s \mathbf{K}_s & \mathbf{B}_s \mathbf{K}_f \\ \mathbf{0} & \frac{\mathbf{A}_f + \bar{\mathbf{B}}_f \mathbf{K}_f}{\epsilon} \end{bmatrix} \begin{bmatrix} \mathbf{z}_s \\ \mathbf{g}_f \end{bmatrix}. \quad (25)$$

Thus, the control input $\mathbf{u} = \mathbf{u}_s + \mathbf{u}_f$ can be expressed as

$$\mathbf{u} = [\mathbf{K}_s \quad \mathbf{0}] \begin{bmatrix} \mathbf{z}_s \\ \mathbf{z}_f \end{bmatrix} + [\mathbf{0} \quad \mathbf{K}_f] \begin{bmatrix} \mathbf{z}_s \\ \mathbf{g}_f \end{bmatrix} = ([\mathbf{K}_s \quad \mathbf{0}] + [\mathbf{0} \quad \mathbf{K}_f] \mathbf{T}_3) \mathbf{Tz} \quad (26)$$

Consequently, composite state feedback gain for the system (17) is given by

$$\hat{\mathbf{K}} = [\mathbf{K}_s + \mathbf{K}_f \mathbf{U} \quad \mathbf{K}_f] \quad (27)$$

Table 2

Eigenvalues of fast subsystem.

Sr. No.	Eigenvalues	Sr. No.	Eigenvalues
1	-7.2484	10	-1.6967×10^2
2	-3.2844×10^1	11	-1.7568×10^2
3	-3.3372×10^1	12	-1.9497×10^2
4	-6.6599×10^1	13	-2.111×10^2
5	-6.8323×10^1	14	-2.1904×10^2
6	-9.3653×10^1	15	-2.3591×10^2
7	-9.4612×10^1	16	-2.7163×10^2
8	-1.0868×10^2	17	-2.7626×10^2
9	-1.1705×10^2		

Table 3

Closed loop eigenvalues of the AHW model.

Sr. No.	Eigenvalues	Sr. No.	Eigenvalues	Sr. No.	Eigenvalues
1	-4.5625×10^{-6}	36	-7.9531×10^{-3}	64	-1.5662×10^{-1}
2–3	$(-3.5399 \pm j 7.7474) \times 10^{-5}$	37	-7.9591×10^{-3}	65	-1.5761×10^{-1}
4	-3.7779×10^{-5}	38–39	$(-9.7370 \pm j 0.11351) \times 10^{-3}$	66	-1.6316×10^{-1}
5	-3.7991×10^{-5}	40	-1.5769×10^{-2}	67	-1.6324×10^{-1}
6–7	$(-3.8092 \pm j 7.6314) \times 10^{-5}$	41	-5.0952×10^{-2}	68	-1.6405×10^{-1}
8–9	$(-6.4915 \pm j 5.2981) \times 10^{-5}$	42	-5.1157×10^{-2}	69	-1.6579×10^{-1}
10–11	$(-6.5894 \pm j 5.4694) \times 10^{-5}$	43	-5.7730×10^{-2}	70	-1.8037×10^{-1}
12–13	$(-7.3379 \pm j 3.9266) \times 10^{-5}$	44	-5.7892×10^{-2}	71	-1.8049×10^{-1}
14–15	$(-7.7423 \pm j 2.9886) \times 10^{-5}$	45	-5.9707×10^{-2}	72	-1.8122×10^{-1}
16–17	$(-8.1067 \pm j 3.8606) \times 10^{-5}$	46	-5.9723×10^{-2}	73	-1.8401×10^{-1}
18–19	$(-8.8817 \pm j 1.8965) \times 10^{-5}$	47	-6.0344×10^{-2}	74	-7.2484
20	-4.0122×10^{-5}	48	-6.0642×10^{-2}	75	-3.2844×10^1
21	-4.1518×10^{-5}	49	-6.1848×10^{-2}	76	-3.3372×10^1
22	-4.2241×10^{-5}	50	-6.1942×10^{-2}	77	-6.6599×10^1
23	-4.4224×10^{-5}	51	-6.2200×10^{-2}	78	-6.8323×10^1
24	-4.7464×10^{-5}	52	-6.2380×10^{-2}	79	-9.3653×10^1
25	-4.8903×10^{-5}	53	-6.2458×10^{-2}	80	-9.4612×10^1
26	-1.4098×10^{-4}	54	-6.2608×10^{-2}	81	-1.0868×10^2
27	-1.4626×10^{-4}	55	-6.2865×10^{-2}	82	-1.1705×10^2
28	-1.5720×10^{-4}	56	-6.2893×10^{-2}	83	-1.6967×10^2
29	-1.6526×10^{-4}	57	-1.1715×10^{-1}	84	-1.7568×10^2
30	-1.6722×10^{-4}	58	-1.4712×10^{-1}	85	-1.9497×10^2
31	-1.7311×10^{-4}	59	-1.4713×10^{-1}	86	-2.1110×10^2
32	-1.8809×10^{-4}	60	-1.4809×10^{-1}	87	-2.1904×10^2
33	-1.8871×10^{-4}	61	-1.4850×10^{-1}	88	-2.3591×10^2
34	-3.3851×10^{-3}	62	-1.5580×10^{-1}	89	-2.7163×10^2
35	-7.9331×10^{-3}	63	-1.5585×10^{-1}	90	-2.7626×10^2

from which, state feedback gain matrix for (11) is obtained as

$$\mathbf{K} = \hat{\mathbf{K}}\mathbf{T}. \quad (28)$$

Applying linear control $\mathbf{u}(t) = \mathbf{K}\mathbf{z}(t)$ to (11), one can get closed loop system as

$$\dot{\mathbf{z}}(t) = (\mathbf{A} + \mathbf{BK})\mathbf{z}(t) \quad (29)$$

which is stable i.e. $(\mathbf{A} + \mathbf{BK})$ has all the eigenvalues in the left half of the s-plane.

Lemma 1. If fast subsystem is asymptotically stable, i.e., $\varphi\left(\frac{\mathbf{A}_f}{\epsilon}\right) < 0$ then state feedback designed for the slow subsystem alone can stabilize the system (11).

Proof. State feedback control law designed for the slow subsystem is given by (19). Closed loop system obtained by applying this control law to the system (17) is given by

$$\begin{bmatrix} \dot{\mathbf{z}}_s \\ \dot{\mathbf{z}}_f \end{bmatrix} = \begin{bmatrix} \mathbf{A}_s + \mathbf{B}_s\mathbf{K}_s & \mathbf{0} \\ \frac{\mathbf{B}_f\mathbf{K}_s}{\epsilon} & \frac{\mathbf{A}_f}{\epsilon} \end{bmatrix} \begin{bmatrix} \mathbf{z}_s \\ \mathbf{z}_f \end{bmatrix}. \quad (30)$$

As $(\mathbf{A}_s + \mathbf{B}_s\mathbf{K}_s)$ is stable by design and $\left(\frac{\mathbf{A}_f}{\epsilon}\right)$ is assumed to be stable, system (30) is stable. Further, system formulation (17) is related to its original form (11) via linear transformation (18). Therefore, system (11) is also stable. \square

Remark 1. If $\varphi\left(\frac{\mathbf{A}_f}{\epsilon}\right) < 0$, then one can assume $\mathbf{K}_f = \mathbf{0}$ in (27), which yields reduced order approximation to $\hat{\mathbf{K}}$ as $\bar{\mathbf{K}} = [\mathbf{K}_s \quad \mathbf{0}]$.

4. Application to spatial control of AHWR

The linear model of the AHWR, given by (9) and (10), is found to be controllable and observable. The control input \mathbf{u} to RR drives consist of two terms, written as

$$\mathbf{u} = \mathbf{u}_{gp} + \mathbf{u}_{sp} \quad (31)$$

where \mathbf{u}_{gp} is global power component, designed in Shimjith et al. (2011a), and \mathbf{u}_{sp} is spatial power feedback component. After application of global and spatial power feedbacks system (9) becomes

$$\dot{\mathbf{z}} = \hat{\mathbf{A}}\mathbf{z} + \mathbf{B}\mathbf{u}_{sp} + \mathbf{B}_{fw}\delta q_{fw} \quad (32)$$

where $\hat{\mathbf{A}}$, given in Shimjith et al. (2011a), has eigenvalues falling in two distinct clusters. First cluster of 73 eigenvalues ranging from -1.8402×10^{-1} to -2.6799×10^{-5} with three eigenvalues at origin

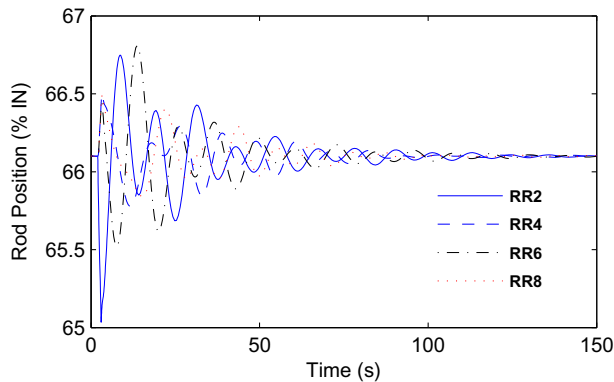


Fig. 2. Variation in RR positions during the transient.

and second cluster of 17 eigenvalues range from -7.2484 to -2.7626×10^2 . Hence, it is possible to transform model (32) into singularly perturbed form (11).

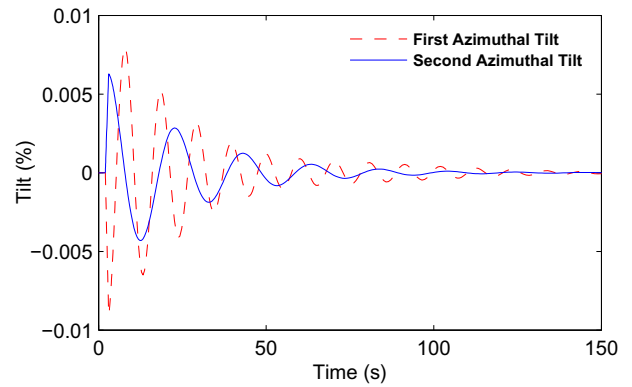


Fig. 3. Suppression of tilts initiated by change in position of RR2.

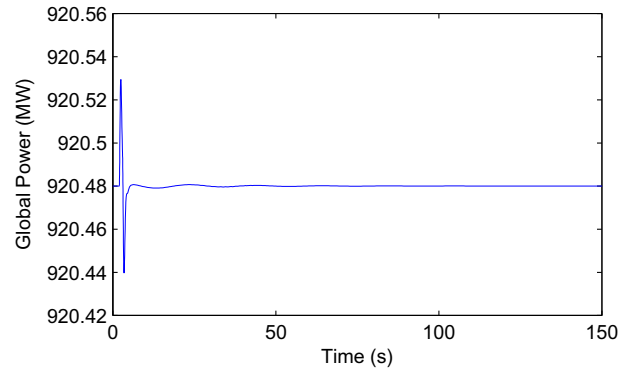


Fig. 4. Variations in global power during the transient.

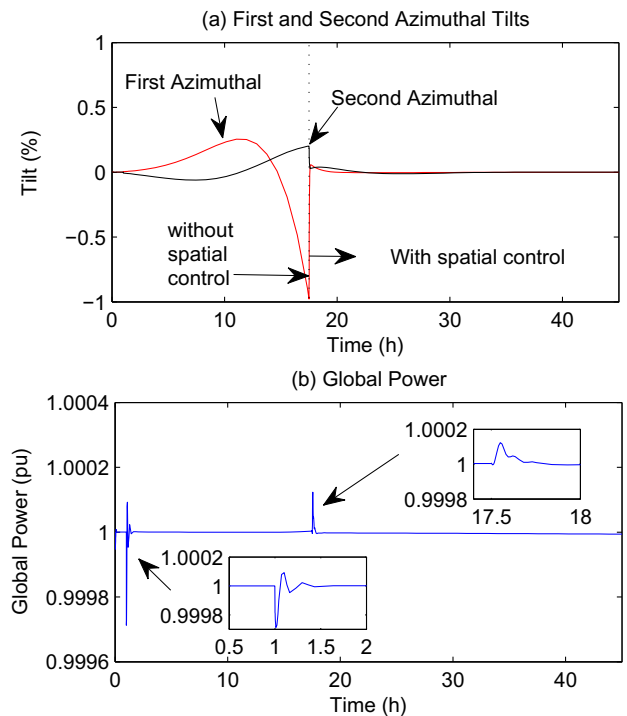


Fig. 5. Suppression of tilts by composite control and corresponding variations in global power.

4.1. Singularly perturbed form of AHWR model

In case of AHWR, after linearization of set of equations given by (1)–(7), it is indeed observed that coefficients in the 17 equations for nodal powers, contain ℓ in their denominator. Its value is 3.6694×10^{-4} s. This parameter can be picked up as ϵ . Therefore, the state variables of system defined by (8) are grouped into slow and fast ones as

$$\mathbf{z}_1 = [\mathbf{z}_H^T \ \mathbf{z}_X^T \ \mathbf{z}_I^T \ \delta h_d \ \mathbf{z}_C^T \ \mathbf{z}_X^T]^T, \quad (33)$$

$$\mathbf{z}_2 = \mathbf{z}_p. \quad (34)$$

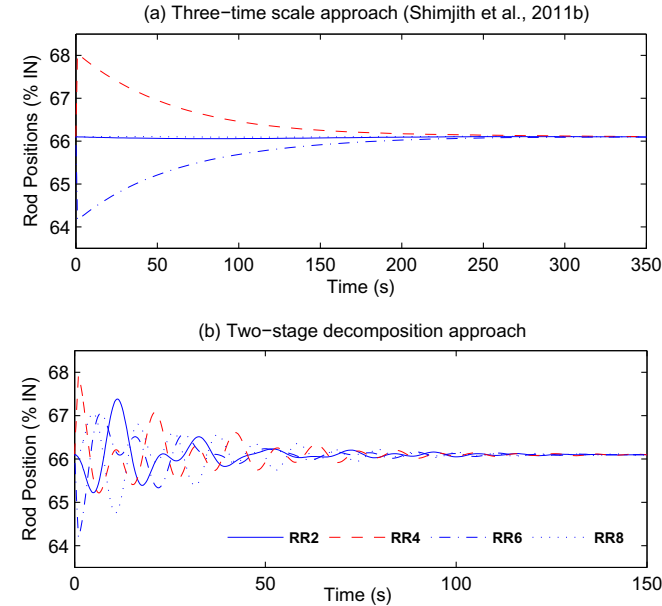


Fig. 6. Comparison of three-time-scale and two-stage decomposition. (See above-mentioned references for further information.)

Now, the AHWR model is transformed into standard singularly perturbed form where $n_1 = 73$ and $n_2 = 17$. Submatrices \mathbf{A}_{11} , \mathbf{A}_{12} , \mathbf{A}_{21} , \mathbf{A}_{22} , \mathbf{B}_1 and \mathbf{B}_2 are respectively of dimensions (73×73) , (73×17) , (17×73) , (17×17) , (73×4) and (17×4) .

4.2. Composite control law

Transformation matrices \mathbf{T}_1 and \mathbf{T}_2 , slow subsystems matrix \mathbf{A}_s and fast subsystem matrix $\frac{\mathbf{A}_f}{\epsilon}$ can be obtained easily by using the procedure explained in Section 3. The eigenvalues of matrices \mathbf{A}_s and $\frac{\mathbf{A}_f}{\epsilon}$ are given in Tables 1 and 2 respectively. It is seen that the eigenvalues of $\frac{\mathbf{A}_f}{\epsilon}$ and \mathbf{A}_s are in excellent agreement with the last 17 and remaining 73 eigenvalues of matrix \mathbf{A} respectively. From Table 2 it can be observed that the eigenvalues of fast subsystem are asymptotically stable i.e. $\phi\left(\frac{\mathbf{A}_f}{\epsilon}\right) < 0$. Hence, composite control law can be constructed using the slow subsystem alone, as given in Lemma 1 and Remark 1. Closed loop eigenvalues of the system with composite control law are given in Table 3.

4.3. Transient simulations

Response of the composite controller was analyzed by simulating the vectorized nonlinear model of AHWR, obtained from (1)–(7), in MATLAB/Simulink environment for the transients involving a disturbance in the spatial power distribution. The reactor was assumed to be initially operating at full power equilibrium condition. Shortly, RR2, originally under auto control, was driven out manually by 1% giving appropriate control signal after 2 s and thereafter left on auto control as shown in Fig. 2. Other RRs moved in under the effect of the controller in order to maintain the total reactor power. After the period during which the manual signal was enforced on RR2, all RRs were being driven by the controller to their original positions within 120 s. Variations in spatial power measured in terms of first and second azimuthal tilts (Munje et al., 2013b), and global power are shown in Fig. 3 and Fig. 4 respectively.

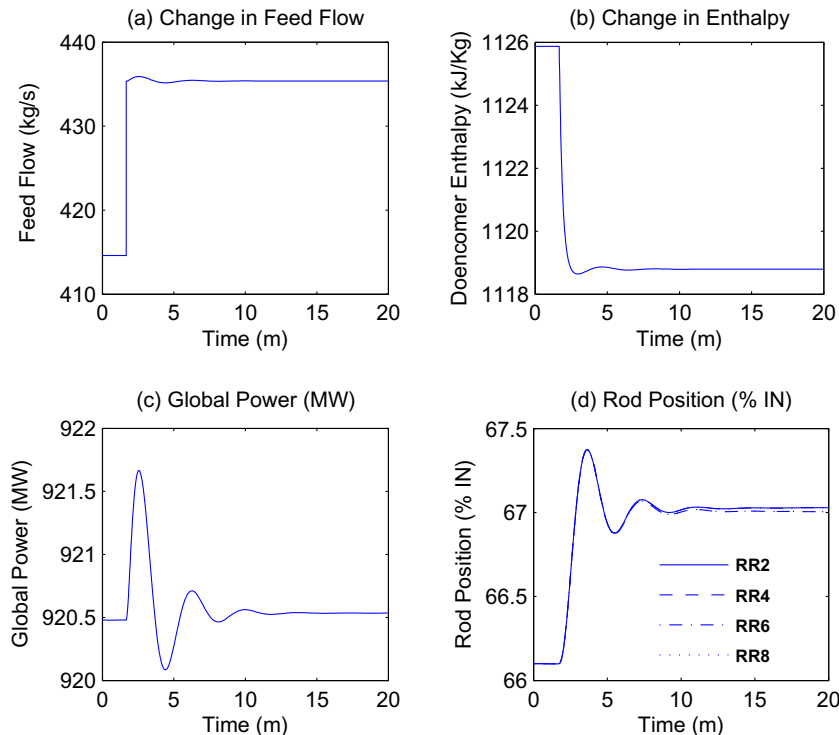


Fig. 7. Effect of 5% positive step change in the feed flow.

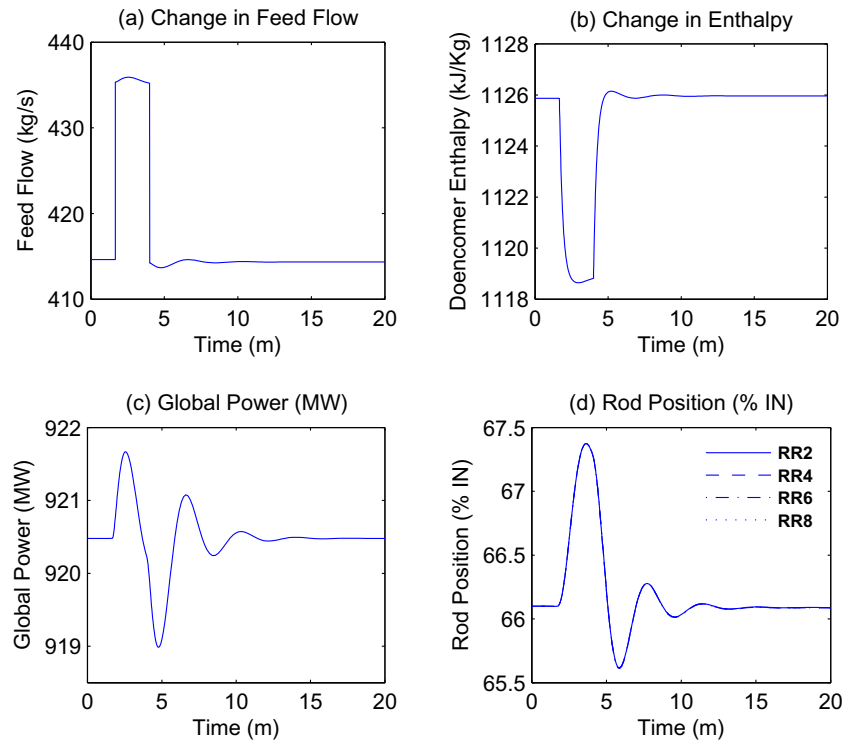


Fig. 8. Effect of temporary disturbance in the feed flow.

Fig. 5 shows the closed loop system response during another transient initiated by a momentary disturbance in position of RR2. It was assumed that reactor was initially operating at full power with the control signal generated by global power feedback, u_{gp} alone. The RR2, which was initially at its equilibrium position was driven in by about 1.5% and immediately driven out to its original position. As a consequence of this disturbance, it was observed that the first and second azimuthal tilts (or modes of xenon-induced spatial oscillations,) started picking up as shown in Fig. 5(a). After about 17.5 h, the spatial control component, u_{sp} was introduced in the control signals. After the introduction of the spatial control component, amplitudes of the tilts are reduced within about 5 m and are completely suppressed in 1.5 h. The tilts remain suppressed thereafter during the remaining prolonged simulation. Fig. 5(b) shows the variations in the global power. It shows variation only when the transient is initiated and when the spatial power component is introduced, elsewhere it remains steady.

Further, the controller is compared with three-time-scale approach presented by Shimjith et al. (2011b). In this case, RR6 was driven out manually by 2% giving appropriate control signal and simultaneously RR4 was driven in by 2%. Immediately after that regulating rods were driven back to their original positions. Result is generated, for variations in control rod positions for both the controllers using the vectorized nonlinear model, as shown in Fig. 6. It is observed that, in both the cases RRs are driven back to their equilibrium positions but time required to do so is less in the suggested controller.

In order to assess the response of the system to disturbance in feed flow, the model was simulated when 5% positive step change was introduced in the feed flow as shown in Fig. 7(a). As a result of this, the incoming coolant enthalpy reduced by about 0.64% (Fig. 7(b)). The total power was found to be stabilizing at its rated value due to the action of controller (Fig. 7(c)). However, RRs are driven in by 0.9% (Fig. 7(d)). For the temporary disturbance introduced in feed flow the total power is found to be stabilizing back at its original value and RRs also came back to their equilibrium positions as illustrated in Fig. 8.

5. Conclusion

In this paper, the original numerically ill-condition system of AHWR is decomposed into two lower order subsystems by two-stage decomposition approach. State feedbacks are then designed for the two subsystems separately and a composite state feedback control for original system is obtained. At the same time composite controller achieves an asymptotic approximation to the closed loop system performance. Performance of the suggested composite controller is judged via simulations carried out under various transient conditions. Proposed controller is also compared with three-time-scale composite controller for same transient levels. It is observed that performance of the suggested controller is better compared to three-time-scale composite controller in terms of spatial stabilization. The control strategy for AHWR, presented here, utilizes the feedback of nodal powers, regulating rods' positions and xenon and iodine concentrations. For the later two variables, it would be necessary to employ an observer or estimator.

Acknowledgements

This work was supported by Board of Research in Nuclear Sciences, Department of Atomic Energy, Government of India under Grant (Sanction No. 2009/36/102-BRNS).

References

- Astrom, K.J., Bell, R.D., 2000. Drum-boiler dynamics. *Automatica* 36, 363–378.
- Chow, J.H., Kokotovic, P.V., 1984. A decomposition of near-optimum regulators for systems with slow and fast modes. *IEEE Trans. Auto. Cont.* 21, 701–705.
- Duderstadt, J.J., Hamilton, L.J., 1975. *Nuclear Reactor Analysis*. John Wiley & Sons Inc., New York.
- Gajic, Z., Lim, M.-T., 2001. *Optimal Control of Singularly Perturbed Linear Systems and Applications: High Accuracy Techniques*. Marcel Dekker, New York, NY, USA.
- Kokotovic, P.V., O'Malley, R.E., Sannuti, P., 1976. Singular perturbation and order reduction in control theory—an overview. *Automatica* 12, 123–132.
- Ladde, G.S., Siljak, D.D., 1983. Multiparameter singular perturbations of linear systems with multiple time scales. *Automatica* 19, 385–394.

- Londhe, P.S., Patre, B.M., Tiwari, A.P., 2014. Design of single-input fuzzy logic controller for spatial control of advanced heavy water reactor. *IEEE Trans. Nucl. Sci.* 61, 901–911.
- Munje, R.K., Londhe, P.S., Parkhe, J.G., Patre, B.M., Tiwari, A.P., 2013. Spatial Control of advanced heavy water reactor by fast output sampling technique. In: *Proc. of IEEE Multi-Conf. on Sys. and Contr.* Hyderabad, India, pp. 1212–1217.
- Munje, R.K., Patre, B.M., Shimjith, S.R., Tiwari, A.P., 2013b. Sliding mode control for spatial stabilization of advanced heavy water reactor. *IEEE Trans. Nucl. Sci.* 60, 3040–3050.
- Munje, R.K., Patre, B.M., Tiwari, A.P., 2014a. Nonlinear simulation and control of xenon induced oscillations in advanced heavy water reactor. *Ann. Nucl. Energy* 64, 191–200.
- Munje, R.K., Patre, B.M., Tiwari, A.P., 2014b. Periodic output feedback for spatial control of AHWR: a three-time-scale approach. *IEEE Trans. Nucl. Sci.* 61, 2373–2382.
- Naidu, D.S., 1988. *Singular Perturbation Methodology in Control Systems*. Peter Peregrinus Ltd., London.
- Patre, B.M., Bandyopadhyay, B., Werner, H., 1997. Control of discrete two time scale system by using piecewise constant periodic output feedback. *Syst. Sci.* 23, 23–37.
- Patre, B.M., Bandyopadhyay, B., Werner, H., 1997. Periodic output feedback control for singularly perturbed discrete model of steam power system. *Proc. IEE Contr. Theory Appl.* 146, 247–252.
- Phillips, R.G., 1980. A two-stage design of linear feedback controls. *IEEE Trans. Auto. Contr.* 25, 1220–1223.
- Saberi, A., Khalil, H., 1985. Stabilization and regulation of nonlinear singularly perturbed systems-composite control. *IEEE Trans. Autom. Contr.* 30, 739–747.
- Saksena, V.R., O'Reilly, J., Kokotovic, P.V., 1984. Singular perturbation and time-scale methods in control theory: survey 1976–1983. *Automatica* 20, 273–293.
- Shimjith, S.R., Tiwari, A.P., Bandyopadhyay, B., 2008. Coupled neutronics–thermal hydraulics model of advanced heavy water reactor for control system studies. *Proc. of IEEE INDICON*, IIT Kanpur, India, pp. 126–131.
- Shimjith, S.R., Tiwari, A.P., Naskar, M., Bandyopadhyay, B., 2010. Space-time kinetics modeling of advanced heavy water reactor for control studies. *Ann. Nucl. Energy* 37, 310–324.
- Shimjith, S.R., Tiwari, A.P., Bandyopadhyay, B., Patil, R.K., 2011a. Spatial stabilization of Advanced Heavy Water Reactor. *Ann. of Nucl. Ener.* 38, 1545–1558.
- Shimjith, S.R., Tiwari, A.P., Bandyopadhyay, B., 2011b. A three-time-scale approach for design of linear state regulator for spatial control of Advanced Heavy Water Reactor. *IEEE Trans. Nucl. Sci.* 58, 1264–1276.
- Shimjith, S.R., Tiwari, A.P., Bandyopadhyay, B., 2011c. Design of fast output sampling controller for three-time-scale systems: application to spatial control of Advanced Heavy Water Reactor. *IEEE Trans. Nucl. Sci.* 48, 3305–3316.
- Sinha, R.K., Kakodkar, A., 2006. Design and development of the AHWR—the Indian Thorium Fuelled Innovative Nuclear Reactor. *Nucl. Eng. Des.* 236, 683–700.
- Suzuki, M., 1981. Composite controls for singularly perturbed systems. *IEEE Trans. Autom. Contr.* 26, 505–507.
- Tiwari, A.P., Bandyopadhyay, B., Govindarajan, G., 1996. Spatial control of a large pressurized Heavy Water Reactor. *IEEE Trans. Nucl. Sci.* 43, 389–402.
- Tiwari, A.P., Bandyopadhyay, B., 1998. Control of xenon induced spatial oscillations in a large PHWR. *Proc. of IEEE Int. Conf. Global Connectivity in Ener., Comp. Communi. and Contr.*, New Delhi, India, pp. 178–181.
- Tiwari, A.P., Bandyopadhyay, B., Werner, H., 2000. Spatial control of large PHWR by piecewise constant periodic output feedback. *IEEE Trans. Nucl. Sci.* 47, 389–402.